Multiphase NiMo with Spatially Separated Active Sites Enabled by Data-Assisted Synthesis for Spillover-Driven Alkaline Hydrogen Evolution Reaction

Raja Rafidah Raja Sulaiman[1], Yichiet Aun[2], Qi Zhang[3], Beibei Tang[3], Ya-Rong Zheng[3], Kee Shyuan Loh[1], Rozan Mohammad Yunus[1], Thye Foo Choo[4], Mohammad Khalid[5,6,7], Wai Yin Wong[1*]

[1]*Fuel Cell Institute, Universiti Kebangsaan Malaysia, 43600 UKM Bangi, Selangor, Malaysia*
[2]*Department of Computer and Communication Technology, Faculty of Information and Communication Technology, Universiti Tunku Abdul Rahman, Jalan Universiti, Bandar Barat, Kampar, Perak, 31900, Malaysia*
[3]*School of Chemistry and Chemical Engineering, Anhui Province Key Laboratory of Value-Added Catalytic Converison and Reaction, Hefei University of Technology, Hefei, 230009, China*
[4]*Malaysian Nuclear Agency, 43000, Kajang, Selangor, Malaysia*
[5]*Materials and Manufacturing Group, James Watt School of Engineering, University of Glasgow, Glasgow G12 8QQ, UK*
[6]*University Centre for Research and Development, Chandigarh University, Mohali, Punjab, 140413, India*
[7]*Faculty of Engineering, Manipal University Jaipur, Rajasthan, 303007, India*

*Corresponding author email: waiyin.wong@ukm.edu.my

Supplementary note 1

Table S1. Configurations for the cubic regressor.

Parameter	Setting
Degree of polynomial	n=3
Input features	Hydrothermal duration (x_1), temperature (x_2)
Feature transformations	Polynomial terms and interactions
Output parameters	Key electrochemical metrics (e.g., overpotential, Tafel slope, Rct)
Optimization criterion	Minimize Sum of Squared Errors (SSE)

The degree-3 polynomial regression equation is expressed as:

$$\hat{y} = \beta_0 + \beta_1 x_1 + \beta_2 x_2 + \beta_3 x_1^2 + \beta_4 x_2^2 + \beta_5 (x_1 \cdot x_2) + \beta_6 x_1^3 + \beta_7 x_2^3 + \beta_8 (x_1^2 \cdot x_2) + \beta_9 (x_1 \cdot x_2^2) \quad \text{(Eq. 2)}$$

Where:

- $\hat{y}$: Predicted electrochemical parameter (e.g., overpotential, Tafel slope).
- x_1: Hydrothermal duration (hours).
- x_2: Hydrothermal temperature (°C).
- $\beta_0, \beta_1, ..., \beta_9$: Coefficients learned during model training.

Evaluation Metrics

To evaluate model accuracy, we use:

- **Mean Squared Error (MSE):** to measures the average squared difference between predicted and actual values, giving higher weight to larger errors.

$$\mathbf{MSE} = (1/n) \Sigma_i (\hat{y}_i - y_i)^2$$

- **Mean Absolute Error (MAE):** to calculates the average of absolute differences between predicted and actual values, offering an interpretable measure of average error.

$$\mathbf{MAE} = (1/n) \Sigma_i |\hat{y}_i - y_i|$$

- **Coefficient of Determination (R^2):** to indicates the proportion of variance in the dependent variable that is predictable from the independent variables, with values closer to 1.0 indicating better fit.

$$\mathbf{R^2} = 1 - \Sigma_i (y_i - \hat{y}_i)^2 / \Sigma_i (y_i - \bar{y})^2$$

Supplementary note 2

Table S2. Summary of the electrochemical HER activity of NiMo/NF electrodes in 1 M KOH.

Electrode	Hydrothermal duration and temperature	η @ 10 mA cm^{-2}	η @ 100 mA cm^{-2}	b (mV/dec)	Rct (Ω)	C_{dl} (F)
NiMo/NF-6-160	6 h, 160 ℃	32.2	126.7	50.5	0.738	17.6
NiMo/NF-6-180	6 h, 180 ℃	30.7	113.8	48.8	0.612	20.9
NiMo/NF-6-200	6 h, 200 ℃	33.0	113.1	51.1	0.580	19.6
NiMo/NF-12-160	12 h, 160 ℃	34.6	147.8	58.9	0.675	17.1
NiMo/NF-12-180	12 h, 180 ℃	31.0	114.8	49.1	0.540	19.7
NiMo/NF-12-200	12 h, 200 ℃	33.0	156.4	56.4	0.882	10.1
NiMo/NF-24-160	24 h, 160 ℃	26.0	121.0	45.7	0.646	28.1
NiMo/NF-24-180	24 h, 180 ℃	28.8	100.5	46.2	0.440	22.0
NiMo/NF-24-200	24 h, 200 ℃	32.8	127.9	49.5	0.446	17.8
NiMo/NF-30-160	30 h, 160 ℃	29.0	142.0	47.6	0.573	12.9
NiMo/NF-30-180	30 h, 180 ℃	30.7	130.3	48.1	0.781	21.4
NiMo/NF-30-200	30 h, 200 ℃	24.1	109.1	43.9	0.554	22.0

Supplementary note 3

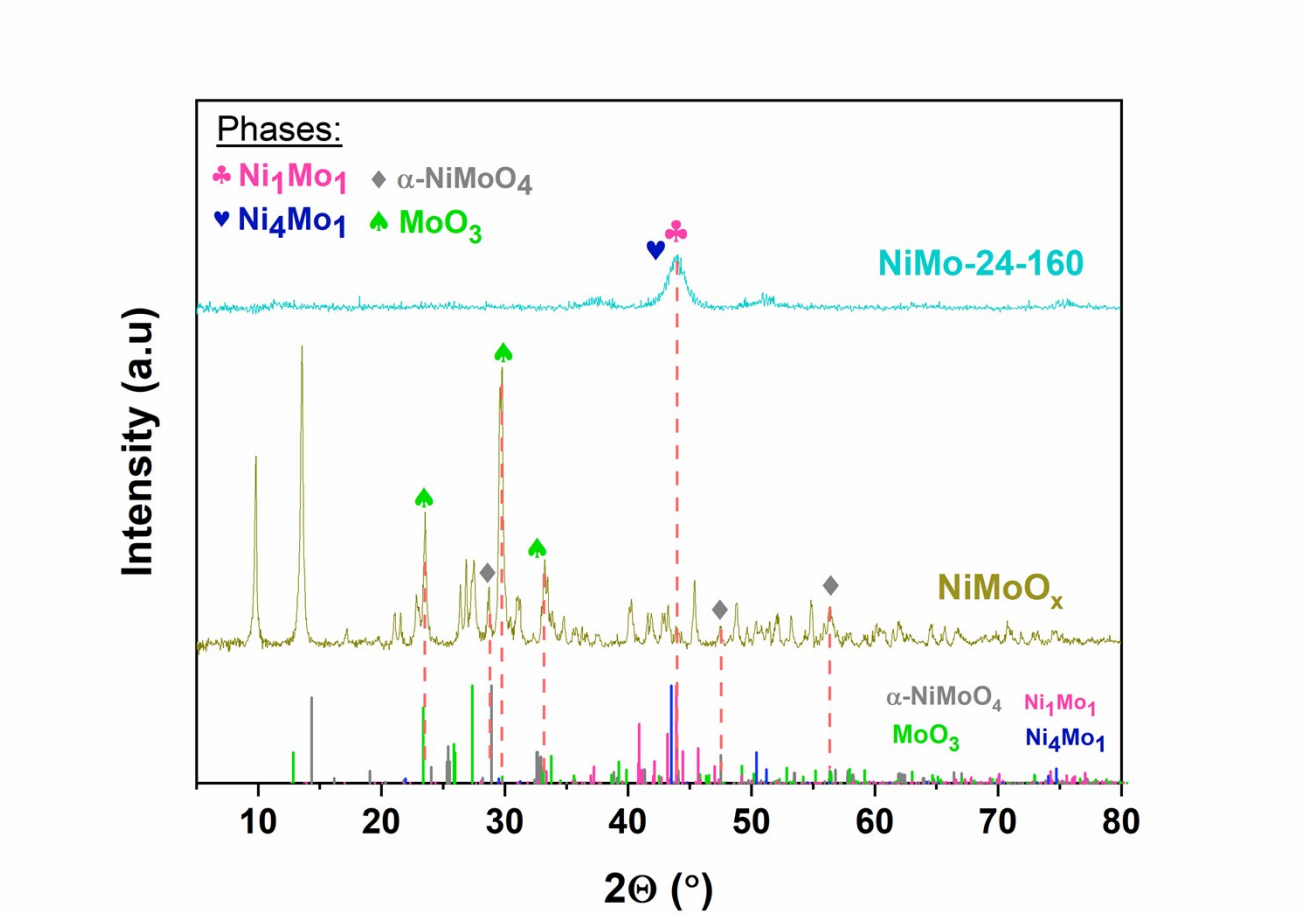

Figure S1. XRD spectra of the non-annealed $NiMoO_x$ with annealed NiMo-24-160.

Supplementary Note 4

Table S3 shows the predictive performance of cubic model using Mean Squared Error (MSE) and the coefficient of determination (R^2). The results show a high degree of accuracy across all electrochemical parameters, ensuring reliable estimations without the need for additional experimental trials. The model achieves MSE values of 0.82 and 0.77 for overpotential at 10 mA/cm² (non-iR and 85%-iR, respectively), indicating minimal deviation from the actual experimental values. The overpotential at 100 mA/cm² (85%-iR) exhibits an MSE of 0.84, which remains within an acceptable range, confirming the model's robustness in capturing trends at higher current densities. Meanwhile, the Tafel slope prediction yields an MSE of 1.27, which, while slightly higher, still indicates strong predictive reliability given the inherent variations in electrochemical kinetics. To smooth extrapolated trends, Gaussian Process Regression (GPR) was used as a post-processing kernel-based interpolator to reduce local oscillations and preserve physical consistency. The application of GPR ensures that interpolated values across unseen parameter ranges maintain physical consistency with experimental observations, thereby extending the applicability of the model without necessitating additional experimental validation. This predictive capability is particularly advantageous for parameter optimization, allowing for informed decision-making in electrode fabrication while minimizing resource-intensive electrochemical testing. Overall, the model demonstrates a high level of predictive accuracy, reducing the need for exhaustive experimental iterations while enabling the rapid screening of optimal synthesis conditions for NiMo/NF electrodes. Note that future work should explore ensemble or Gaussian process models to quantify predictive uncertainty and identify dominant interaction effects. This would enhance interpretability and guide synthesis optimization under sparse data regimes.

Table S3. Summary of the model evaluation analysis.

	MSE	**R^2 Score**
Overpotential @ 10 mA cm^{-2} (non-iR)	0.81809324	0.897655878
Overpotential @ 10 mA cm^{-2} (85%-iR)	0.771538462	0.901485634
Overpotential @ 100 mA cm^{-2} (85%-iR)	0.84	0.873724884
Tafel Slope (mV dec^{-1})	1.27	0.875809172

Supplementary Note 5

Table S4. Single-cell performance comparison with literature studies including NiMo-based cathodes in AAEMWE.

Anode	Cathode	MEA fabrication	Electrolyte, temperature	Single-cell performance			Half-cell HER activity	
				Cell voltage (V_{cell})	Current density (mA/cm^2)	Cell stability	Overpotential (mV) @ j ($mA\ cm^{-2}$)	Tafel slope ($mV\ dec^{-1}$)
$NiFe_2O_4$/SS felt	NiMo/NF-24-160 (This work)	Method: Binder-free CCS Substrate: NF AEM: Fumasep® FAA-3-50	1 M KOH, 60 °C	1.99 – 2.02	400.2	100 h, 400 mA cm^{-2}: Overall stable around 2 V_{cell} with little potential fluctuation.	26.0 @ 10 mA cm^{-2} 121.0 @ 100 mA cm^{-2}	45.7
$NiFe_2O_4$/SS felt	NiMo/NF-24-180 (This work)	Method: Binder-free CCS Substrate: NF AEM: Fumasep® FAA-3-50	1 M KOH, 60 °C	2.02 – 2.05	401.0	50 h, 400 mA cm^{-2}: Higher initial cell potential stabilizing around 2 V_{cell}.	28.8 @ 10 mA cm^{-2} 100.5 @ 100 mA cm^{-2}	46.2
$Co_2(OH)_3Cl$/ FeOOH	MoNi/ $NiMoO_x$ [1]	Method: CCS, binder-free Substrate: NF AEM: Fumasep® FAA-3-PK-130	1 M KOH, 30 °C	~2.23	200.0	1600 h, 200 mA cm^{-2}: Overall stable with slight fluctuations. No significant increase in cell potential around 2.2 V_{cell}.	9 @ 10 mA cm^{-2}	31

Fe-NiMo-NH_3/H_2	NiMo-NH_3/H_2 [2]	Method: CCS, not binder-free. Nafion binder supported on CP and NF used. Substrate: CP AEM: Sustainion® X37-50	1 M KOH, 80 °C	1.57	1000	25 h, 500 mA cm^{-2}: Initial cell potential around 1.7 V_{cell} slowly increasing over time.	11 @ 10 mA cm^{-2} 107 @ 500 mA/cm^2	28
NF	$MoO_{3-x}NiMoO_4$/ NF [3]	Method: CCS, not binder-free. Catalyst ink prepared in the presence of Vulcan XC-72 carbon and PSEBS-CM ionomer. Substrate: NF Membrane: Fumasep ®FAA-3-PK-130	1 M KOH, 60 °C	~2.2	820	50 h, 1000 mA cm^{-2}: Oscillation between 2.2 V_{cell}. Voltage increase observed to occur faster towards the end.	-	75

References

[1] X. Shi, X. Zheng, H. Wang, H. Zhang, M. Qin, B. Lin, M. Qi, S. Mao, H. Ning, R. Yang, L. Xi, Y. Wang, Hierarchical Crystalline/Amorphous Heterostructure MoNi/NiMoOx for Electrochemical Hydrogen Evolution with Industry-Level Activity and Stability, Adv. Funct. Mater. 33(41) (2023) 2307109. https://doi.org/https://doi.org/10.1002/adfm.202307109.

[2] P. Chen, X. Hu, High-Efficiency Anion Exchange Membrane Water Electrolysis Employing Non-Noble Metal Catalysts, Advanced Energy Materials 10(39) (2020) 2002285. https://doi.org/https://doi.org/10.1002/aenm.202002285.

[3] F. Bartoli, C. Castello, T. Peruzzolo, E. Berretti, E. Sediva, K. Bouzek, J. Hnát, M. Plevova, L. Poggini, H.A. Miller, MoO3-xNiMoO4 nanorods synthesized using NiO nanoparticles for hydrogen evolution in anion exchange membrane water electrolysis, Chem. Eng. J. 511 (2025) 162026. https://doi.org/https://doi.org/10.1016/j.cej.2025.162026.